Available online at www.sciencedirect.com

ScienceDirect

Procedia CIRP 58 (2017) 422 – 427

www.elsevier.com/locate/procedia

16th CIRP Conference on Modelling of Machining Operations

Estimation of Dynamic Grinding Wheel Wear in Plunge Grinding

M. Ahrens[a*], J. Damm[b], M. Dagen[a], B. Denkena[b], T. Ortmaier[a]

[a] *Leibniz Universität Hannover, Institute of Mechatronic Systems, Appelstraße 11a, 30167 Hannover, Germany*
[b] *Leibniz Universität Hannover, Institute of Production Engineering and Machine Tools (IFW), An der Universität 2, 30823 Garbsen, Germany*

* *Markus Ahrens. Tel.: +49 511 / 762-17843; Fax:+49 511 / 762-19976. markus.ahrens@imes.uni-hannover.de.*

Using conventional grinding wheels, self-excited vibrations are one of the most limiting factors in terms of productivity and process stability in cylindrical plunge grinding. Depending on the dynamic behavior of the workpiece and machine, vibrations of the workpiece copy on the grinding wheel's surface, caused by uneven wear. This results in increasing waviness of the grinding wheel and by that, increasing workpiece vibration. Electromagnetic actuators are capable of influencing the dynamic process forces and therefore, the wear. The authors pursue the objective, to achieve an active control of the tool wear for low workpiece vibration and high workpiece quality. Therefore, a tool-wear-model which enables the estimation of the grinding wheel's surface is proposed. The parameterization of the model is realized carrying out a set of reference processes with subsequent identification. Aside from the dynamic tool wear, the workpiece oscillation is simulated by the model. A Kalman Filter is utilized to adjust the model onto the current process using the measured workpiece oscillation. Thus, it is possible to achieve an online estimation of the wave amplitude and phase angle on the grinding wheel's surface as well as their progression.

Peer-review under responsibility of the scientific committee of The 16th CIRP Conference on Modelling of Machining Operations

Keywords: Grinding, Monitoring, Regenerative Chatter, Modelling

1. Introduction

Finishing processes like grinding are used to achieve high surface quality or low tolerance in manufacturing. Compared to other processes like turning or milling, the material removal rate of grinding is relatively low which results in high process duration and cost-intensive processes. Thus, this costly process only is carried out, if the demands on a workpiece require it, making the economic efficiency of the grinding process an important factor. The production of a flawless workpiece may suffer from vibrations of internal or external sources. Internal disturbance is often caused by self-exited oscillations, also called chatter. Especially conventional abrasives like corundum grinding wheels tend to develop vibrations due to wheel-sided regenerative effect. Contrary to the workpiece-sided regenerative effect, where vibrations occur due to an increasingly wavy workpiece surface, the wheel-sided regenerative effect is caused by waves forming on the grinding wheel's surface. Vibrations of the workpiece copy onto the wheel due to varying contact force and tool wear. The uneven tool excites the workpiece's oscillation even more, causing an increasing waviness on the grinding wheel with every revolution. Even at low amplitudes below one micron, surface waves excite dynamic process forces and may damage the machine as well as the workpiece as they increase. The waves on the wheel have to be removed by time consuming dressing operations, limiting the economic efficiency of the grinding process.

The mechanism and development of chatter vibration has been part of various researches, many of them focusing on modeling the grinding process. In 1969 Snoeys & Brown [1] presented one of the first feedback process models relying on grinding forces, workpiece displacement and tool wear, see Figure 1. Many more recent models are based on this schematic, cf. Inasaki [2] and Weck [3]. Other approaches like Schütte [4] concentrate on the physical processes during grinding, taking geometric-kinematic, microscopic tool properties, temperatures, etc. into account, sometimes using FEM. Brinksmeyer et al. reviewed existing models and compared the complexity, usability and computational cost in [5].

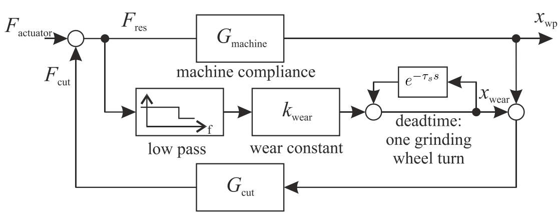

Figure 1: Simplified Grinding Process Model for Wheel-Sided Chatter Vibration in Time Domain by Snoeys & Brown, cf. [1]

Peer-review under responsibility of the scientific committee of The 16th CIRP Conference on Modelling of Machining Operations
doi:10.1016/j.procir.2017.03.247

When it comes to modeling wheel-sided chatter vibration, most of the existing models suffer from the high effort of parameter setting, as the dynamic behavior of the machine as well as various process parameters are required for good model quality.
In this paper, a simplified grinding process model is presented, which targets the development of wheel sided chatter vibration and on the estimation of workpiece movement and tool wear. The authors pursue the objective, to achieve an active control of the tool wear, applying forces on the workpiece using a magnetic actuator [6]. After description of the model structure, the measurement setup is presented. An exemplary grinding process is carried out during which wheel sided chatter is deliberately induced by a magnetic actuator. This process is used for the identification of model parameters. A Kalman filter is utilized for online-estimation of the tool surface waviness during grinding processes.

2. Measurement and Actuation Setup

Figure 2 shows the measurement setup used for the experiments conducted in this paper. While the model only depends on the workpiece position measurement provided by eddy current sensors, various other sensors are implemented for validation. Besides acoustic emission, the tool position, tailstock acceleration, workpiece forces, and spindle current are measured. The magnetic actuator depicted in Figure 3 is able to apply forces onto the workpiece.

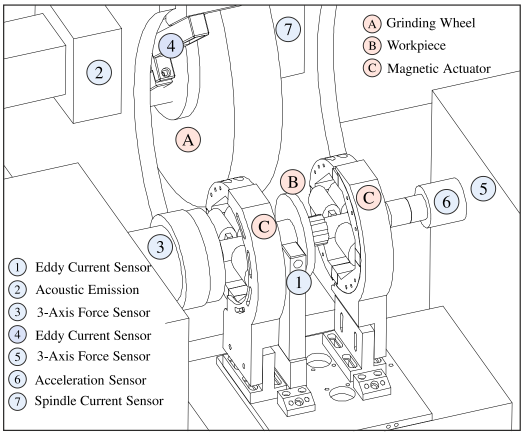

Figure 2: Measurement Setup

2.1. Grinding Machine

The experiments presented in this paper are performed on a SCHAUDT CR41 CBN, being a CNC type cylindrical plunge-grinding machine with automatic balancing system and belt driven spindle. It is equipped with hydrostatic guide ways and screw drives enhancing the damping and stiffness of the machine. To obtain comparable results, a standardized grinding process is defined. The workpiece consists of bearing steel (C100Cr6 / 1.3505 at 62HRC) in form of 10 mm wide disks with a diameter of 100 mm on a shaft of 200 mm length. The used grinding wheel is composed of white aluminum oxide at grain size F120 (FEPA) with bond hardness H and slightly porous structure. The deployed cooling fluid is mineral oil at 45 ℓ/min. Running the process at a cutting velocity of v_c =35 $\mathrm{m/s}$, a speed ratio q = 80, and a specific material removal rate Q'_w = 5 $\mathrm{mm^3/mm\ s}$ results in a slightly instable process with slow developing chatter [7].

2.2. Electromagnetic Actuator

The grinding process is influenced by the magnetic actuator depicted in Figure 3. The actuators are able to generate forces of ± 30 N at adjustable angle. The magnet's iron cores are 30 mm wide and composed of laminated soft magnetic material to reduce losses due to eddy currents and ensure high dynamics of the actuator. The current in the magnet coils is controlled by Junus servo amplifiers connected to a 160 V intermediate circuit. [8] Using a pseudo-random-bit-sequence-signal (prbs), its dynamic behavior can be identified as a PT_1-system with corner frequency at 700 Hz and 0.2 ms delay. Thus, it is possible to reach up to 15 N at 1 kHz. The highest chatter frequencies ocouring in the presented setup are roughly at 1.1 kHz [9]. The actuator and the sensors are connected to a DSPACE ds1103 process computer system with a sample time of $t_s = 10^{-4}$s.

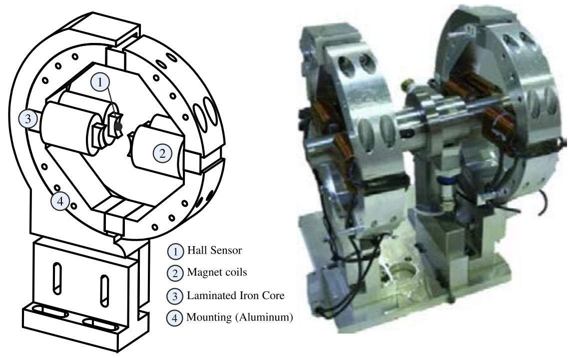

Figure 3: Electromagnetic Actuator CAD model (left) and Prototype (right)

3. Modelling of Wheel-sided Chatter Vibration

The proposed model focuses on the simulation of the development of wheel-sided chatter vibrations, i. e. the formation of waves on the grinding wheel due to tool wear. Since these waves can only form at multiples of the grinding wheels revolution frequency, the modelling can be split up in n different models, each representing a discrete frequency, covering the frequency range in which chatter vibrations may occur. Since the waves develop relatively slow, the transfer functions of the dynamic behavior of the machine as well as the dynamic cutting compliance depicted in Figure 1 simplify to a quasi-static modulation of amplitude and phase-shift of the signal. Utilizing complex numbers, the transfer functions are reduced to a multiplication with a constant complex value, cf. Figure 4.

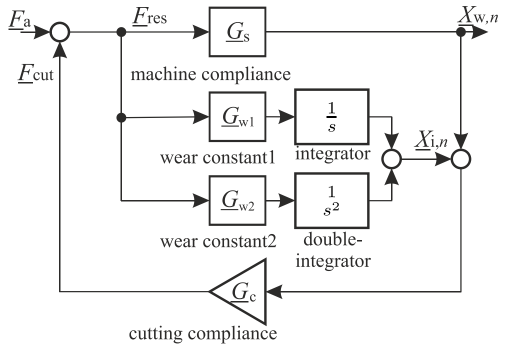

Figure 4: Grinding Process Model for Wheel Sided Chatter in Frequency Domain for a single frequency $k\dot{\varphi}_{gw}$

In this model $\underline{G}_s$ represents the machine's compliance and $\underline{G}_c$ the dynamic cutting compliance. The input of the model is the actuator force $\underline{F}_a$ resulting in a workpiece oscillation $\underline{X}_{w,n}$. The tool wear, often modeled by a dead time element, is represented by a set of integrators, adding up the forces applied to the wheel's surface multiplied by the wear parameters $\underline{G}_{w1}$ and $\underline{G}_{w2}$. An underlined variable indicates a complex number. The transfer function of the model is given by

$$\frac{\underline{X}_{w,n}}{\underline{F}_a} = \frac{\underline{G}_s s^2}{(1-\underline{G}_s\,\underline{G}_c)s^2 - \underline{G}_c\,\underline{G}_{w1} s - \underline{G}_c\,\underline{G}_{w2}}. \quad (1)$$

For a given model output and input force, the sum of the integrator state i. e. the wheels waviness $\underline{Xi}_k$ can be calculated by:

$$\underline{X}_{i,n} = \underline{X}_{w,n}\,\frac{1-\underline{G}_s\,\underline{G}_c}{\underline{G}_s\,\underline{G}_c} - \frac{\underline{F}_a}{\underline{G}_s}. \quad (2)$$

Thus, it is possible to describe expected workpiece movement and the underlying wheel surface for a given input force. The model can also be expressed in a state space representation:

$$\underline{\boldsymbol{A}} = \begin{bmatrix} 0 & 1 \\ \frac{\underline{G}_c\,\underline{G}_{w2}}{1-\underline{G}_s\,\underline{G}_c} & \frac{\underline{G}_c\,\underline{G}_{w1}}{1-\underline{G}_s\underline{G}_c} \end{bmatrix},$$

$$\underline{\boldsymbol{B}} = \begin{bmatrix} 1 \\ 0 \end{bmatrix}, \quad (3)$$

$$\underline{\boldsymbol{C}} = \begin{bmatrix} \frac{\underline{G}_s\underline{G}_c\,\underline{G}_{w2}}{1-\underline{G}_s\,\underline{G}_c} & \frac{\underline{G}_s\underline{G}_c\,\underline{G}_{w1}}{1-\underline{G}_s\,\underline{G}_c} \end{bmatrix},$$

$$\underline{\boldsymbol{D}} = \underline{G}_s.$$

The first order approximation of the discrete state space model at a sample time of t_s is given by:

$$\underline{\boldsymbol{A}}_d = \boldsymbol{I} + \boldsymbol{A}\cdot t_s,$$

$$\underline{\boldsymbol{B}}_d = \underline{\boldsymbol{B}}\cdot t_s, \quad (4)$$

$$\underline{\boldsymbol{C}}_d = \underline{\boldsymbol{C}},$$

$$\underline{\boldsymbol{D}}_d = \underline{\boldsymbol{D}},$$

where $\underline{\boldsymbol{A}}_d$, $\underline{\boldsymbol{B}}_d$, $\underline{\boldsymbol{C}}_d$ and $\underline{\boldsymbol{D}}_d$ represent the discrete state space matrices and $\boldsymbol{I}$ the identity matrix.

4. Identification of the Process Model Parameters

4.1. Tool Wear dynamics

Figure 5 shows how the waves generate on the grinding wheel's surface. Since the incremental wear Δx_i per grinding wheel turn is small compared to the wave amplitudes forming over time, the phase angle difference $\Delta\varphi_i$ between the existing wave and the actual wear is determining the wave development. Phase angles between $\frac{\pi}{2} < \Delta\varphi_i < \frac{3\pi}{2}$ cause the waves to grow over time, outside of this interval the waves will be reduced. Angels of $\Delta\varphi_i \neq m\,\pi,\ m \in \mathbb{N}$, will cause the waves to move along the perimeter of the wheel.

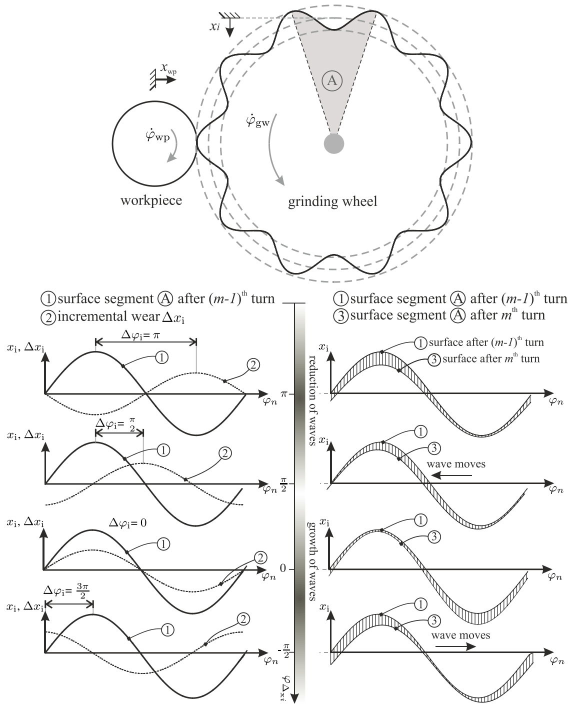

Figure 5: Dynamic Wear on the Grinding Wheel, cf. [3]

In the following, the model's dynamic is identified. The model has two sources of excitation, the external force represented by the magnetic actuator and the internal force provided by the integrator states, i. e. the waves on the grinding wheel. At the beginning, the tool wear is zero, corresponding to a freshly dressed tool. In a first stage, oscillations are induced by the actuator, causing the formation of waves on the grinding wheel. In the second stage, the generated waves contribute further to the excitation of workpiece oscillation causing the wheel's surface to change further, see Figure 6.

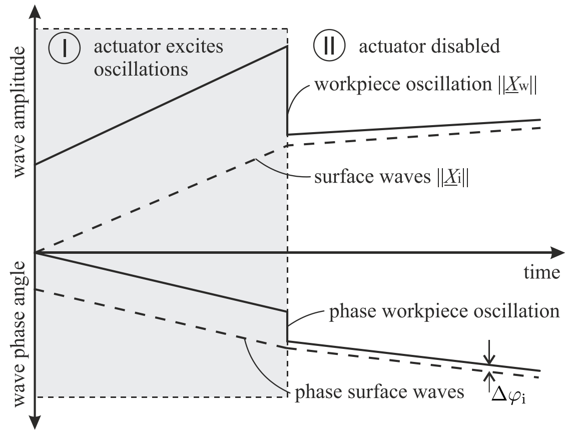

Figure 6: Sketch of Workpiece Oscillation and Surface Wave Progression Excited by the Electromagnetic Actuator

After some time the actuator is switched off and the process is only exited by the waves on the grinding wheels surface. If the phase angle $\Delta\varphi_i$ of the incremental tool wear Δx_i is in the area of $\frac{\pi}{2} < \Delta\varphi_i < \frac{3\pi}{2}$, the excitation of the surface waves leads to an increased wave amplitude, cf. Figure 5.

4.2. Parameter identification

For identification purpose, a reference process (cf. section 2.1) is carried out. From the start of the process, the actuator applies a force at a discrete frequency – which is a multiple of the wheel's rotation speed – for 10 seconds on the workpiece. The measured workpiece oscillation x_{wp} is split up into amplitude and phase of n frequencies using a discrete frequency model:

$$\hat{x}_{wp} = \sum_{n=W_1}^{W_2} a_n \sin(n\varphi_{gw}) + b_n \cos(n\varphi_{gw}). \qquad (5)$$

A recursive least squares (rls) algorithm, detailed description in [10], estimates the parameters a_n and b_n, where φ_{gw} is the wheel's angle, n the multiple of the rotation speed and $[W_1, W_2]$ the interval of frequencies that are estimated. The amplitude A_n, the phase angle φ_n and their corresponding complex expression $\underline{X}_{w,n}$ are given by

$$A_n = \sqrt{a_n^2 + b_n^2},$$

$$\varphi_n = \mathrm{atan2}(b_n, a_n), \text{and} \qquad (6)$$

$$\underline{X}_{w,n} = A_n \, e^{j\varphi_n}.$$

Figure 7 depicts the output of the rls algorithm $\underline{X}_{w,n}$ and the progression of amplitudes and phase angles during a reference process excited by an exemplary chosen frequency of n = 30 at $\dot{\varphi}_{gw}$ = 194.8 $\frac{\text{rad}}{\text{s}}$.

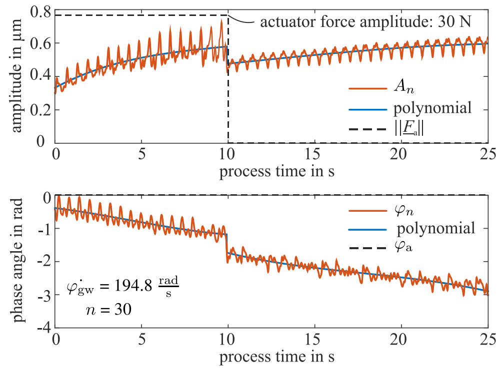

Figure 7: Recursive Least Squares (rls) Algorithm Output of a Reference Process Excited by the Magnetic Actuator with a Force of 30 N at approx. 930 Hz (n = 30)

The measurement is heavily distorted due to the unroundness of the measuring area beneath the workpiece and therefore, shows an overlying periodic signal. To cancel out this effect, a 3[rd] order polynomial is fitted into the data. The result is used as reference data and represents the desired model output. The model parameter vector $\boldsymbol{p}_n$ is given by

$$\underline{\boldsymbol{p}}_n = \begin{bmatrix} \underline{G}_s \\ \underline{G}_c \\ \underline{G}_{w1} \\ \underline{G}_{w2} \end{bmatrix}. \qquad (7)$$

A Nelder-Mead simplex algorithm is deployed for calculation of optimal model parameters.

5. Estimation of Wheel's Surface and Model Validation

5.1. Kalman Filter

The model does not cover the excitation due to the process itself, which is responsible for the generation of the initial waves when grinding without the additional actuator. Thus, a Kalman Filter is employed to reduce these modelling errors and on the other hand smoothing the measured data, cf. Figure 8.

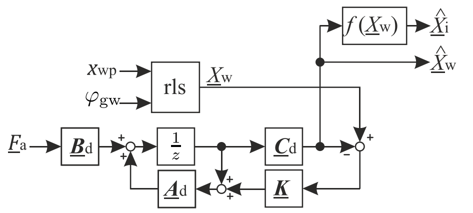

Figure 8: Block Diagram of Surface Estimation using a Kalman Filter and Recursive Least Squares (rls) Algorithm

The Kalman Gain $\boldsymbol{K}$ in a time step k can be calculated by:

$$\underline{\hat{\boldsymbol{P}}}_{k+1} = \underline{\boldsymbol{A}}_d \underline{\boldsymbol{P}}_k \underline{\boldsymbol{A}}_d^T + \boldsymbol{Q}$$

$$\underline{\boldsymbol{K}}_{k+1} = \underline{\hat{\boldsymbol{P}}}_{k+1} \underline{\boldsymbol{C}}_d^T \left(\underline{\boldsymbol{C}}_d \, \underline{\hat{\boldsymbol{P}}}_{k+1} \, \underline{\boldsymbol{C}}_d^T + R \right)^{-1}, \qquad (8)$$

$$\underline{\boldsymbol{P}}_{k+1} = (\boldsymbol{I} - \underline{\boldsymbol{K}}_{k+1}) \underline{\hat{\boldsymbol{P}}}_{k+1}.$$

The covariance matrix $\boldsymbol{Q} = \boldsymbol{I} \cdot 10^{-3}$ and sensor covariance $R = 10^{-5}$ were chosen in a way, that the measurement effects the estimation just enough to set the model states on the right operating point. The output of the filter gives an estimation of the workpiece oscillation $\underline{\hat{X}}_{w,n}$ and surface waves $\underline{\hat{X}}_{\mathrm{i},n}$

5.2. *Surface reconstruction for validation*

To evaluate the performance and integrity of the model, the estimated surface is compared to the real surface topography of the grinding wheel. Since the measurement of wheels waviness is difficult and time intensive – no matter if during the process or post-process – an alternative method has been carried out [9].
By using a modified dressing process, it is possible to calculate the surface. The wheel is dressed in steps of one micron at a low overlap factor. The acoustic emission (AE) signal is mapped on the wheel's angle φ_{gw} and added up. A sine function of the corresponding frequency is fitted to the signal using a Least Square algorithm to smooth the reconstructed surface. Figure 9 shows the AE signal amplitude and the fitted sine function $\underline{\tilde{X}}_{\mathrm{i},n}$.

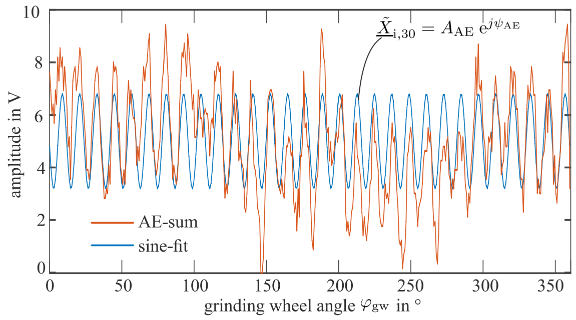

Figure 9: Reconstruction of Grinding Wheel Surface using AE-Signal-Mapping

Since the amplitude A_{AE} of the sine-fit is only based on the AE signal intensity, it has no direct physical correspondence to the wave amplitude. However, the excitation frequency of $n = 30$ can clearly be identified and the phase angle ψ_{AE} of the signal coincides with the wheel's surface. Thus, it can be used as an indicator for the model quality by comparison of the angles of surface estimation $\underline{\hat{X}}_{\mathrm{i},n}$ and surface reconstruction $\underline{\tilde{X}}_{\mathrm{i},n}$.

6. Results

The proposed setup with the identified model is now deployed in another process for testing and validation. Like in the previous process, the actuator is used to generate waves on the grinding wheel at a discrete frequency. The workpiece oscillation $\underline{\hat{X}w}_k$ and surface waves $\underline{\hat{X}}_{\mathrm{i},n}$ depicted in Figure 10 are estimated by the Kalman Filter online during the process.

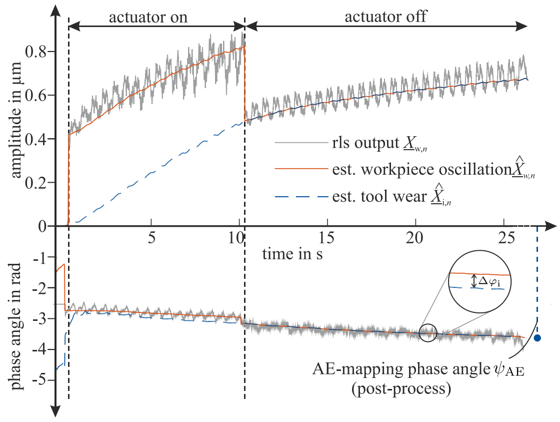

Figure 10: Test of the Setup with Validation Process

It can be seen, that the estimated waves on the tool are almost congruent to the workpiece oscillation when the excitation by the actuator is absent. However, the workpiece movement is not identical to the surface. There is a small difference $\Delta\varphi_{\mathrm{i}}$ which is responsible for the wave progression and decreasing phase angle over time. When the actuator is switched on, it creates a step in the workpiece oscillation. Due to the freshly dressed tool, there are no waves on wheel's surface. Thus, the wear's amplitude $\underline{\hat{X}}_{\mathrm{i},n}$ starts at zero and rises during the process. When the actuator is switched off, the process is solely excited by the waves and both estimations draw near each other. After the process an AE-mapping described in section 5.2 is carried out. The phase angle of the reconstructed surface ψ_{AE} is represented by the dot at the end of the process. It can be seen, that the angle of the estimated surface meets the angle of the AE, which supports the conclusion, that the estimated surface is reliable. The parameter identification and validation process is carried out for each n in the interval of $[24,\ 34]$ and shows good results comparable to those presented here for $n = 30$. Outside of this interval, the process stability is higher and thus, the wave generation is too small to get reliable results.

7. Conclusion

Wheel-sided chatter vibration are a limiting factor in plunge grinding, when it comes to the economic production of high quality workpiece surfaces by plunge grinding. Thus, the authors developed an electromagnetic actuator to influence the grinding process and prevent chatter vibration. In this paper a model for estimation of workpiece movement and tool wear during a plunge grinding processes is proposed. Thus, a controller can be developed, to apply forces that depend directly on the estimated tool surface and enable the reduction of waves on the tool. Instead of modelling the process in time domain, the task is split up in a small number of more simple models in frequency domain. This simplification can entail small inaccuracies at the beginning of the process, when the wave amplitudes are not equally distributed along the wheels perimeter. However, after a few wheel revolutions these deviations vanish. The model is parametrized during a reference process and combined with a Kalman Filter. Thus, it is robust with respect to small parameter changes. However, bigger parameter changes require the reference process to be performed once more. Therefore, automatic and online identification of the proposed model as well as the development of a tool wear controller will be part of future work.

8. Acknowledgement

The authors thank the German Research Foundation (DFG) for supporting this project.

9. References

[1] Snoeys, R.; Brown, D.: Dominating Parameters in Grinding Wheel- and Workpiece Regenerative Chatter, Proceedings of the 10th International Machine Tool Design and Research Conference, 1969

[2] Inasaki, I.: Grinding Process Simulation Based on the Wheel Topography Measurement, CIRP Annals - Manufacturing Technology 45, Nr. 1, pp. 347 – 350, 1996

[3] Weck, M.; Brecher, C.: Werkzeugmaschinen 5: Messtechnische Untersuchung und Beurteilung, dynamische Stabilität, Springer Verlag, 7. Auflage, 2006

[4] Schütte, O.; Heimann, B: On the Dynamics of Chatter Vibrations in External Cylindrical Grinding, Procedia of the 8th ISROMAC Congress, pp. 892-900, Honolulu, 2000

[5] Brinksmeier, E.; Aurich, J.C.; Govekar, E.; Heinzel, C.; Hoffmeister, H.-W.; Klocke, F.; Peters, J.; Rentsch, R.; Stephenson, D.J.; Uhlmann, E.; Weinert, K.; Wittmann, M.: Advances in Modeling and Simulation of Grinding Processes, CIRP Annals - Manufacturing Technology 55, no. 2, pp. 667 – 696, 2006

[6] Ahrens, M.; Fischer, R.; Dagen, M.; Denkena, B.; Ortmaier, T.: Active Chatter Damping in Plunge Grinding using Magnetic Actuators, Proceedings of the ASME 2014 International Manufacturing Science and Engineering Conference, MSEC2014, June 9-13, Detroit, Michigan, USA, 2014

[7] Ahrens, M.; Dagen, M.; Denkena, B.; Ortmaier, T.: An Active Damping Method for Chatter Vibration in Plunge Grinding using Electromagnetic Actuators,7th CIRP Conference on High Performance cutting, Procedia CIRP Volume 46, pp. 197-200, 2016

[8] Copley Controls product brochure Junus JSP-180-30, copleycontrols.com/Motion/pdf/Junus.pdf, 12/2016

[9] Ahrens, M.; Fischer, R.; Dagen, M.; Denkena, B.; Ortmaier, T.: Abrasion Monitoring and Automatic Chatter Detection in Cylindrical Plunge Grinding, 14th CIRP Conference on Modeling of Machining Operations, Procedia CIRP Volume 8, pp. 374-378, 2013

[10] Denkena, B., Ortmaier, T., Ahrens, M., Fischer, R.: Monitoring of Grinding Wheel Defects using Recursive Estimation, The International Journal of Advanced Manufacturing Technology, Volume 75, Issue 5, pp 1005-1015, 2014